Shear Wave Imaging Framework for Quantification of Myocardial Tissue Properties

Martin S Andersen[1], Peter Søgaard[2], Samuel E Schmidt[1], Johannes J Struijk[1]

[1]Aalborg University, Aalborg, Denmark
[2]Aalborg University Hospital, Aalborg, Denmark

Abstract

Analysis of myocardial and arterial wall tissue properties can potentially be used to diagnose cardiovascular pathophysiology. Many cardiovascular diseases, such as Left Bundle Branch Block, Myocardial Infarcts and arteriosclerosis alters tissue elasticity. A known analogue to tissue elasticity is the velocity of the propagating shear waves through tissue, which can be quantified non-invasively as shear wave velocity, derived from ultrasound Shear Wave Imaging (SWI). Developing new SWI techniques require custom programming and a deep knowledge of research-based ultrasound systems. A SWI framework was developed to identify natural shear waves in 800ms windows and generate an acoustic radiation force pulse for generating artificial shear waves in tissue, for use in linear and phased array setups. The MATLAB code and setup framework are provided as an open-source package made available on GitHub. To verify the SWI framework, Acoustic Radiation Force, followed by SWI were made in a tissue mimicking ultrasound phantom. Shear waves propagated at $2.71 \pm 0.12\ m/s$*, which did not vary significantly with respect to neither scan depth (P=0.77) nor tissue attenuation (P=0.88). The framework can potentially be useful for aspiring researchers starting their work in SWI imaging using the Verasonics Vantage System.*

1. Introduction

One of the holy grails of cardiology is eletro-mechanical coupling of the heart [1], [2]. Electrically, some of the most important work done dates to the 70's, where Durrer et al. 1970 described the excitation propagation patterns of the human heart, describing the path the electrical wavefront takes through the cardiac Atrium and Ventricle [3]. Similar mapping of mechanical cardiac contraction has been difficult, as the mechanical movement varies significantly between patients[4].

Shear Wave Imaging (SWI) is a modality that can be used for describing changes to tissue property using a doppler approach to describing changes [5]. SWI therefore has multiple potential clinical applications within cardiovascular imaging, such as the potential to describe the mechanical contractile wavefront [1]. The SWI modality use doppler shift between acquisitions to detect shear waves, and hence can detect very small deformations in tissues, that would be otherwise undetectable [6]. These shear waves can occur though for a natural physiological event, such Mitral Valve opening or closing, that naturally cannot be controlled by the operator, and are therefore called natural shear waves [7]–[9]. The shear waves can be created by the operator as well, where one of the most well-known methods uses the transducer itself to generate acoustic pressure. When shear waves are imaged using shear waves generated by the transducer, this is known as Acoustic Radiation Force Imaging (ARFI) [10], [11]. ARFI generates a prolonged transmit pulse, for lasting for a duration of about 1000 wavelengths, that generates tension in the focused tissue. The tissue will return to a relaxed state, at the cessation of the pulse, which in turn generates a small shear wave, which propagates perpendicular to the transmit pulse, originating at the origin of the ARFI pulse [11]. Natural shear wave amplitudes are normally a factor of magnitude larger than ARFI [7]. ARFI is dependent on the transducer to generate the shear waves, ARFI is severely limited in both penetration depth, but also dependent on not having any natural shear waves occur during acquisition [12]. When using ARFI, the operator is in complete control of when and where the shear waves originate from [6].

While several challenges persist for SWI and ARFI, the modalities could breach the gap for in-vivo electromechanical coupling[1]. However, we are not quite there yet. Furthermore, the learning curve for new researchers to develop new SWI and ARFI methodologies are initially steep, and documentation somewhat limited.

In this paper, a framework for better understanding one of the more developed systems for ultrasound research, the Verasonics Vantage System (Vantage), and to provide new researchers a good starting point for developing new SWI and ARFI methodologies.

2. Methods

The Verasonics Ultrasound system consists of a Host controller or computer (Host), and the Vantage system. It is the programmer's task to tell both the Host and Vantage system how data is to be recorded, and how, when and what data will be transferred to the Host.

Receive Buffer

The scan depth (r) describes how far into tissue you wish to scan. For phased arrays this is generally defined as the maximum tissue depth with respect to the center of the transducer. The Receive Buffer size require the maximum scan depth (r') for the radio frequency (RF) data to be considered. to be used for memory allocation, which is dependent on r, the aperture width (a), which are both generally measured in wavelengths, and the field of view (fov), see Figure 1, and is defined using the law of cosines:

$$r' = \sqrt{\left(\frac{a}{2}\right)^2 + r^2 - a \cdot r \cdot \cos\left(\frac{fov + \pi}{2}\right)}$$

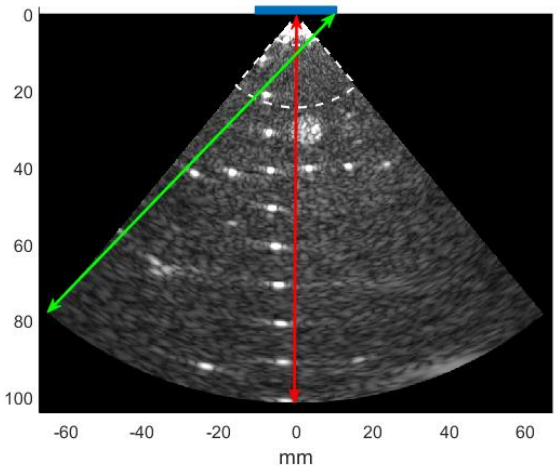

Figure 1 illustrates a B-mode image of an ultrasound phantom. Here the red arrow corresponds the TX/RX scan depth with respect to the center of the transducer. The green arrow describes the scan depth (r') needed for memory allocation due to the longest TX/RX operation, which is dependent of the transducer aperture width, here marked by the blue square at the top of the figure, and field of view. Note that r' will never exceed $r + a/2$, where a is with width of the aperture.

The sound wave roundtrip defines how much memory should be allocated per subframe acquisition of the radio frequency (RF) data. This is calculated as the length of the entire roundtrip (r_{rt}):

$$r_{rt} = 2 \cdot r'$$

When allocating resources for the Receive buffer rows are defined in 128 sample intervals, so the allocated memory of the Receive buffer is defined as:

$$n_{rowsPerFrame} = ceil\left(r_{rt} \cdot n_{spw} \cdot 2^{-7}\right) \cdot 2^7 \cdot n_a \cdot n_p$$

Where n_{spw} is samples per wavelength, n_a is number of subframes, n_p is number of pages per frame.

Pixel Data Object

The Pixel Data Object (PData) is used to define the fov of the transducer field. This will provide the pixel size of the IQ data, using the PDelta field, where $[\Delta\theta, \Delta r, 0]$ describe pixel size in polar coordinates in angles and wavelengths. The Size field contains the size of each subframe in the receive buffer and is defined as $[n_{rows}, n_{cols}, 1]$, where n_{rows} and n_{cols} are defined as:

$$n_{rows} = ceil\left(\frac{r}{\Delta r}\right), \qquad n_{cols} = ceil\left(\frac{fov}{\Delta\theta}\right)$$

Note, that the last element defines the elevation size. And must be 1, and not 0. If set to 0, no errors will be identified, but at run time, MATLAB will crash due to illegal memory access.

Sequence Control Object

The Sequence Control object contains several fields. The primary field is the command field, where you tell the Host and Vantage system a specific task to do, such as 'timeToNextAcq', which is self-explanatory, and require an argument, of how long the Vantage System should wait between transmit/receive (TX/RX) operations. The argument here is defined in *ns*, and the theoretical limit as to how often the Verasonics System could generate new TX/RX operations to achieve a certain framerate (FR) is defined by the pulse repetition frequency (T_{prf}) by:

$$T_{prf} = \frac{r_{rt} \cdot \lambda}{c}, \qquad FR = \frac{c}{r_{rt} \cdot \lambda}$$

Where λ is the wavelength, c is the speed of sound in tissue, and defined as $c = 1.54 \frac{mm}{\mu s}$.

Shear Wave Images

The external functions are where SWI data is generated from the complex In-phase Quadrature (*IQ)* data. The 1-lag autocorrelation (R_1), is a complex number, and can be calculated for every *IQ*-pixel between sequential acquisitions, using the equation:

$$R_1(n) = IQ(n) \cdot IQ(n-1)^*$$

Where IQ^* is the complex conjugate of IQ, and n is the acquisition number. Then the SWI is as:

$$SWI = \angle R_1 \cdot \frac{v_{nyq}}{2\pi}$$

Where, $\angle R_1$ is the angle of R_1, and v_{nyq} is the Nyquist velocity, which is the maximum velocity the system is capable of measuring, and therefore also known as the velocity limit, defined by:

$$v_{nyq} = \frac{c}{2f_0 T_{prf}}$$

Where f_0 is the central frequency, T_{prf} is the repetition frequency of the acquisitions. To avoid sampling-aliasing it is the programmer's task to ensure that T_{prf} is sufficient. For example, using a transducer with a central frequency of $f_c = 3MHz$, and a frame rate of 1000 fps ($T_{prf} = 1ms$) sampling-aliasing will occur when tissue movement exceed 26 cm/s.

Acoustic Radiation Force Imaging

The transmit waveform object (TW) then provides the information required for the Vantage system to generate the ARFI push. For initial purposes, the TW object can be defined as the following:

$$\text{TW} = \begin{Bmatrix} type: & 'Parametric' \\ Parameters: & [f_0, b, n_{cycles} \cdot 2, p] \end{Bmatrix}$$

Where, b is the on-time for every half cycle with $b = 0.67$ will approximate a sine wave, n_{cycles} is the number of wave-cycles for the ARFI push, and p is the polarity of the first half-cycle.

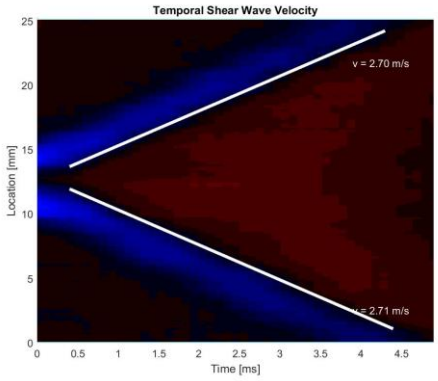

Figure 2 show a temporal shear wave image, where shear waves are identified over a 25 mm window, with the ARFI push located at the center, at a scan depth of 15 mm. Two wave fronts were identified propagating away from the Origin at velocities of 2.70 m/s and 2.71 m/s respectfully.

The External Function and Process

For custom processing, external functions and Process' are required. In the presented script, this function handle will generate a SWI. The Process defines which data buffer, and what source buffer should be transferred to which external function, i.e., 'inter' will preprocess the RF data, and transfer the *IQ* data, to the external function.

Script & Analysis

For illustrative purposes, a ARFI script has been presented, and made available to the reader on GitHub. It generates a trigger signal from the ultrasound system at the onset of each ARFI pulse, allowing for control of external IO devices. The script allows the user to activate ARFI. The function also defines an external function extProcessIQ function, where SWI's are generated. We refer to the GitHub repository for the specific implementation of the *processIQ* function.

To verify system performed as expected, a tissue mimicking phantom (CIRS Model 040GSE) was used. Here the ARFI push was generated at 9 different places, with three different measurements at scan depths of 15mm, 30mm, and 45 mm at both high (0.95 dB/cm/MHz) and low (0.7 dB/cm/MHz) medium attenuation. The propagating velocity was calculated from a temporal shear wave image. The identified shear wave propagation velocity was recorded and analyzed with a two-way ANOVA.

3. Results

The presented script generated an ARFI push and detecting the resulting shear waves at different scan depths between 15mm and 45mm. Velocities of $v_{15mm} = 2.74 \pm 0.08\,{}^{m}/_{s}$, $v_{30mm} = 2.72 \pm 0.13\,{}^{m}/_{s}$, and $v_{45mm} = 2.73 \pm 0.16\,{}^{m}/_{s}$ were measured, see Table 1. They did not show significant differences with respect to scan depth (P=0.77) or medium attenuation (P=0.88), see Table 2. The propagation velocity deviation increased, with a standard deviation of $0.16\,{}^{m}/_{s}$ compared to $0.08\,{}^{m}/_{s}$ at a 45mm and 15mm scan depth respectfully, see Table 1. This was due to the ARFI push pressure decrease as a function of scan depth, see Figures 2 and 3.

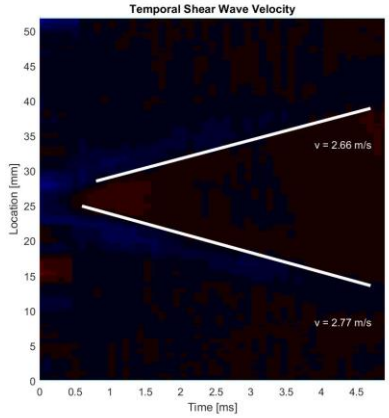

Figure 3 show a temporal shear wave image, where shear waves are identified over a 52 mm window, with the ARFI push located at the center, at a scan depth of 45 mm. Two wave fronts were identified propagating away from the Origin at velocities of 2.66 m/s and 2.77 m/s respectfully.

4. Discussion

The inherent entry level learning curve is steep for new researchers who wish to delve into electromechanical coupling of the heart. This has already been addressed to a degree by hardware vendors providing the researcher with great development platforms. While several examples are made available online for the researcher, these examples can be difficult to understand without prior knowledge of the vendor specific platform. In this manuscript a framework for the Verasonics Vantage System was developed. This can in the future be used as a general foundation of researching Naturally occurring and ARFI generated shear waves. This framework produces ARFI generated shear waves which can be identified without being significantly affected by scan depth.

Attenuation		$0.7\frac{dB}{cm\ MHz}$	$0.7\frac{dB}{cm\ MHz}$
Scan depth	15mm	$2.73 \pm 0.06\frac{m}{s}$	$2.65 \pm 0.06\frac{m}{s}$
	30mm	$2.66 \pm 0.17\frac{m}{s}$	$2.77 \pm 0.06\frac{m}{s}$
	45mm	$2.70 \pm 0.13\frac{m}{s}$	$2.72 \pm 0.12\frac{m}{s}$
	Total	$2.70 \pm 0.13\frac{m}{s}$	$2.72 \pm 0.12\frac{m}{s}$

Table 1 show the detected shear wave velocities in at different scandepths and attenuations.

Two-way ANOVA

	F	P
Depth	0,259	0,774
Attenuation	0,023	0,881

Table 2 show the results of the two-way ANOVA. No significant differences were identified for the factors Depth or Medium Attenuation.

References

[1] O. Villemain *et al.*, "Ultrafast Ultrasound Imaging in Pediatric and Adult Cardiology: Techniques, Applications, and Perspectives," *JACC Cardiovasc Imaging*, vol. 13, no. 8, pp. 1771–1791, 2020, doi: 10.1016/j.jcmg.2019.09.019.

[2] M. v. Andersen *et al.*, "Quantitative Parameters of High-Frame-Rate Strain in Patients with Echocardiographically Normal Function," *Ultrasound Med Biol*, vol. Article in, no. 00, pp. 1–11, 2019, doi: 10.1016/j.ultrasmedbio.2018.11.007.

[3] D. Durrer, R. T. van Dam, G. E. Freud, M. J. Janse, F. L. Meijler, and R. C. Arzbaecher, "Total excitation of the isolated human heart.," *Circulation*, vol. 41, no. 6, pp. 899–912, 1970, doi: 10.1161/01.CIR.41.6.899.

[4] L. M. Swift, M. W. Kay, C. M. Ripplinger, and N. G. Posnack, "Stop the beat to see the rhythm: Excitation-contraction uncoupling in cardiac research," *American Journal of Physiology - Heart and Circulatory Physiology*, vol. 231, no. 6. American Physiological Society, pp. H1005–H1013, Dec. 01, 2021. doi: 10.1152/ajpheart.00477.2021.

[5] A. Caenen *et al.*, "Assessing cardiac stiffness using ultrasound shear wave elastography," *Phys Med Biol*, vol. 67, no. 2, p. 02TR01, Jan. 2022, doi: 10.1088/1361-6560/ac404d.

[6] K. Nightingale, M. S. Soo, R. Nightingale, and G. Trahey, "Acoustic radiation force impulse imaging: in vivo demonstration of clinical feasibility," *Ultrasound Med Biol*, vol. 28, no. 2, pp. 227–235, 2016, doi: 10.1016/S0301-5629(01)00499-9.

[7] M. Strachinaru *et al.*, "Naturally Occurring Shear Waves in Healthy Volunteers and Hypertrophic Cardiomyopathy Patients," *Ultrasound Med Biol*, vol. 45, no. 8, pp. 1977–1986, Aug. 2019, doi: 10.1016/j.ultrasmedbio.2019.04.004.

[8] P. Santos *et al.*, "Natural Shear Wave Imaging in the Human Heart: Normal Values, Feasibility, and Reproducibility," *IEEE Trans Ultrason Ferroelectr Freq Control*, vol. 66, no. 3, pp. 442–452, 2019, doi: 10.1109/TUFFC.2018.2881493.

[9] C. Papadacci, V. Finel, O. Villemain, M. Tanter, and M. Pernot, "4D Ultrafast Ultrasound Imaging of Naturally Occurring Shear Waves in the Human Heart," *IEEE Trans Med Imaging*, vol. 39, no. 12, pp. 4436–4444, Dec. 2020, doi: 10.1109/TMI.2020.3020147.

[10] K. Nightingale, "Acoustic Radiation Force Impulse (ARFI) Imaging: A Review," *Curr Med Imaging Rev*, vol. 7, no. 4, pp. 328–339, Nov. 2011, doi: 10.2174/157340511798038657.

[11] M. L. Palmeri and K. R. Nightingale, "Acoustic radiation force-based elasticity imaging methods," *Interface Focus*, vol. 1, no. 4, pp. 553–564, 2011, doi: 10.1098/rsfs.2011.0023.

[12] P. Santos *et al.*, "Natural shear wave imaging in the human heart: normal values, feasibility and reproducibility," *IEEE Trans Ultrason Ferroelectr Freq Control*, vol. 66, no. 3, pp. 442–452, 2019, doi: 10.1109/TUFFC.2018.2881493.

Address for correspondence:
Martin Siemienski Andersen
Fredrik Bajers Vej 7E,
9220 Aalborg, Denmark.
mvan@hst.aau.dk